CONTENTS

	Page	
ABSTRACT	1	1/A6
1. INTRODUCTION	1	1/A6
2. LIQUID LEVEL DETECTORS	3	1/A8
2.1 Tests of Prototype HTCs	4	1/A9
2.1.1 Test facility	4	1/A9
2.1.2 Description of probe	4	1/A9
2.1.3 Test description	6	1/A11
2.2 Procurement and Fabrication of HTC Sensors	8	1/A13
2.2.1 Procurement of naval reactor-type sensors	8	1/A13
2.2.2 ORNL fabrication	8	1/A13
2.3 Loop-Current-Step-Response Tests	10	1/B1
2.4 THTF Fluid Thermocouple Signal Analysis	13	1/B5
2.5 Thermal-Hydraulic Model of HTC Level Test	13	1/B5
2.6 Ultrasonic Method	13	1/B5
2.7 Contacts with Utilities and Reactor Vendors	14	1/B6
3. SIGNAL ANALYSIS STUDIES WITH DRAG FLOWMETERS	15	1/B7
3.1 Methods	15	1/B7
3.2 Results	17	1/B10
4. VORTEX SHEDDING FLOWMETER	20	1/B14
4.1 Description of Test Meter	21	1/C1
4.2 Test Methods	23	1/C3
4.3 Results	24	1/C4
4.3.1 Single-phase flow	25	1/C5
4.3.2 Two-phase flow	25	1/C5
4.4 Vortex Flowmeter Summary and Recommendations	34	1/D3
REFERENCES	35	1/D4

JUN 2 1980

Item 105-H-11 43.N88:25/1346

ornl

OAK RIDGE NATIONAL LABORATORY

UNION CARBIDE

NUREG/CR-1346
ORNL/NUREG/TM-382

COMPLETED ORIGINAL

Advanced Two-Phase Flow Instrumentation Program Quarterly Progress Report for October-December 1979

K. G. Turnage
C. E. Davis
R. L. Anderson
G. N. Miller

OPERATED BY
UNION CARBIDE CORPORATION
FOR THE UNITED STATES
DEPARTMENT OF ENERGY

Prepared for the U.S. Nuclear Regulatory Commission
Office of Nuclear Regulatory Research
Under Interagency Agreements DOE 40-551-75 and 40-552-75

Printed in the United States of America. Available from
National Technical Information Service
U.S. Department of Commerce
5285 Port Royal Road, Springfield, Virginia 22161

Available from

GPO Sales Program
Division of Technical Information and Document Control
U.S. Nuclear Regulatory Commission
Washington, D.C. 20555

This report was prepared as an account of work sponsored by an agency of the United States Government. Neither the United States Government nor any agency thereof, nor any of their employees, makes any warranty, express or implied, or assumes any legal liability or responsibility for the accuracy, completeness, or usefulness of any information, apparatus, product, or process disclosed, or represents that its use would not infringe privately owned rights. Reference herein to any specific commercial product, process, or service by trade name, trademark, manufacturer, or otherwise, does not necessarily constitute or imply its endorsement, recommendation, or favoring by the United States Government or any agency thereof. The views and opinions of authors expressed herein do not necessarily state or reflect those of the United States Government or any agency thereof.

NUREG/CR-1346
ORNL/NUREG/TM-382
Dist. Category R2

Contract No. W-7405-eng-26

Engineering Technology Division

ADVANCED TWO-PHASE FLOW INSTRUMENTATION PROGRAM QUARTERLY PROGRESS REPORT FOR OCTOBER–DECEMBER 1979

K. G. Turnage R. L. Anderson
C. E. Davis G. N. Miller

Manuscript Completed – April 10, 1980
Date Published – May 1980

NOTICE This document contains information of a preliminary nature. It is subject to revision or correction and therefore does not represent a final report.

Prepared for the
U.S. Nuclear Regulatory Commission
Office of Nuclear Regulatory Research
Under Interagency Agreements DOE 40-551-75 and 40-552-75

NRC FIN No. B0401

Prepared by the
OAK RIDGE NATIONAL LABORATORY
Oak Ridge, Tennessee 37830
operated by
UNION CARBIDE CORPORATION
for the
DEPARTMENT OF ENERGY

BLANK PAGE

ADVANCED TWO-PHASE FLOW INSTRUMENTATION PROGRAM QUARTERLY PROGRESS REPORT FOR OCTOBER–DECEMBER 1979

K. G. Turnage R. L. Anderson
C. E. Davis G. N. Miller

ABSTRACT

Experiments and analysis performed to develop reliable coolant level sensors for in-core use in light-water power reactors are described. Studies during this period involved use of thermal-type sensors and ultrasonic devices. Signal analysis studies of drag flowmeters at 62-cm separation have provided additional data on the feasibility of cross-correlation for two-phase flow velocity measurements. A completed feasibility study of the use of an enhanced vortex shedding flowmeter for making measurements in two-phase flow is described. The conclusion was reached that the vortex shedding mechanism is severely limited for two-phase flow application.

---

1. INTRODUCTION

A primary objective of the Advanced Two-Phase Flow Instrumentation (ATPI) Program is to develop reliable coolant level sensors for in-core use in light-water power reactors. Two concepts are being pursued concurrently: heated thermocouple (HTC) arrays and ultrasonic techniques. Detectors are being designed, fabricated, and tested before proceeding to the design of prototype instruments for in-core or in-reactor use. The emphasis of this task is to develop reliable level detectors which can be retrofitted into existing plants and incorporated into new reactor designs.

The ATPI Program is also involved in hardware development and application of instrument signal correlation and noise analysis to two-phase flow measurements required in reactor safety research. Hardware development includes feasibility studies of novel instruments (such as vortex shedding meters) for application in two-phase flow measurements. The noise analysis studies presently center on the application of analysis techniques for determining velocity and void fraction of two-phase flows under conditions thought to be typical of a nuclear reactor reflood. Both

local impedance probes and full-flow instruments have been used in these experiments.

During the current report period, progress was made in several areas. Scoping tests of prototype HTC liquid level devices were performed in the Transient Instrument Test Facility (TITF). Preparation for future level detector evaluation is proceeding. Additional cross-correlation experiments were performed with two drag flowmeters in two-phase air-water flow. For those tests the instrument separation was 62 cm, significantly greater than for previous tests. A series of experiments, which were performed to examine the feasibility of vortex shedding flowmeters for making measurements in two-phase flow, were completed and documented.

2. LIQUID LEVEL DETECTORS

R. L. Anderson* G. N. Miller*
K. G. Turnage†

To date, the development of level detectors includes the following accomplishments.

1. Modification and shakedown of the TITF for testing of level sensors has been implemented.
2. An HTC level sensor was tested in the TITF in both constant-current and current-controlled modes.
3. An order for ten HTC liquid level sensor assemblies has been placed with Robinson Halpern Company, the manufacturer of liquid level sensors for the U.S. Naval Reactors Program. Two second-generation HTC prototypes were designed and fabricated at Oak Ridge National Laboratory (ORNL).
4. Experiments were performed in the TITF with a sheathed thermocouple using the loop-current-step-response technique.
5. Thermocouple signals from the in-bundle array rod were recorded during bundle boiloff tests performed in the Thermal-Hydraulic Test Facility (THTF). Analogue recordings obtained are suitable for signal analysis.
6. A RELAP4 computer model of the TITF pressurizer and the HTC liquid level probe was prepared and debugged.
7. A 3-m-long ribbon-type ultrasonic sensor was successfully tested as a level indicator at room temperature.
8. Discussions have been held with electric utility [i.e, Tennessee Valley Authority (TVA)] and reactor vendor personnel regarding installation requirements for in-vessel instrumentation and near-term proposals for making level measurements in pressurized water reactors.

---

*Instrumentation and Controls Division.

†Engineering Technology Division.

2.1 Tests of Prototype HTCs

2.1.1 Test facility

The TITF was chosen for the scoping tests of prototype HTCs because it met the basic requirement of providing a high-temperature (up to 300°C) saturated steam/water interface and it was readily available. (The facility was built primarily for testing of instrumented piping spool pieces under high-temperature transient conditions, particularly blowdowns.[1]) For level probe testing, the system is pressurized using strip heaters mounted on the pressurizer body; then the level sensors under test (Fig. 1) are covered and uncovered with saturated water using system letdown valves and a high-pressure injection pump.

An accurate indication of the pressure level, obtained independently of the sensor(s) under test, is definitely required. Water level in the pressurizer is monitored using pressure taps and water-filled tubes (Fig. 1) connected to a differential pressure (dp) cell liquid level transducer. During preliminary testing the indicated pressurizer level was affected unreasonably when the absolute pressure in the system was varied. Modifications to the dp level system were made to assure completely water-filled lines. The dp transducer was recalibrated against a standard, and a second pressure transducer was installed parallel to the dp cell to verify the accuracy of its reading. The effects of the weight of steam at higher pressures and of variations in the saturated water density were taken into account in calibrating the dp cell readout for use at high temperatures.

2.1.2 Description of probe

Initial tests were performed with a prototype HTC liquid level detector fabricated using four-wire metal-sheathed magnesium-oxide-insulated material of 3 mm diam for the lead wires. The sensor assembly was contained in a capsule brazed to the end of the lead-wire assembly. Thermocouple wires were strung through a length of two-hole hard-fired alumina insulator and attached to the matching Chromel and Alumel wires in the lead assembly. The heater was wound onto the surface of the alumina insulator and attached to two nickel-plated copper leads in the lead

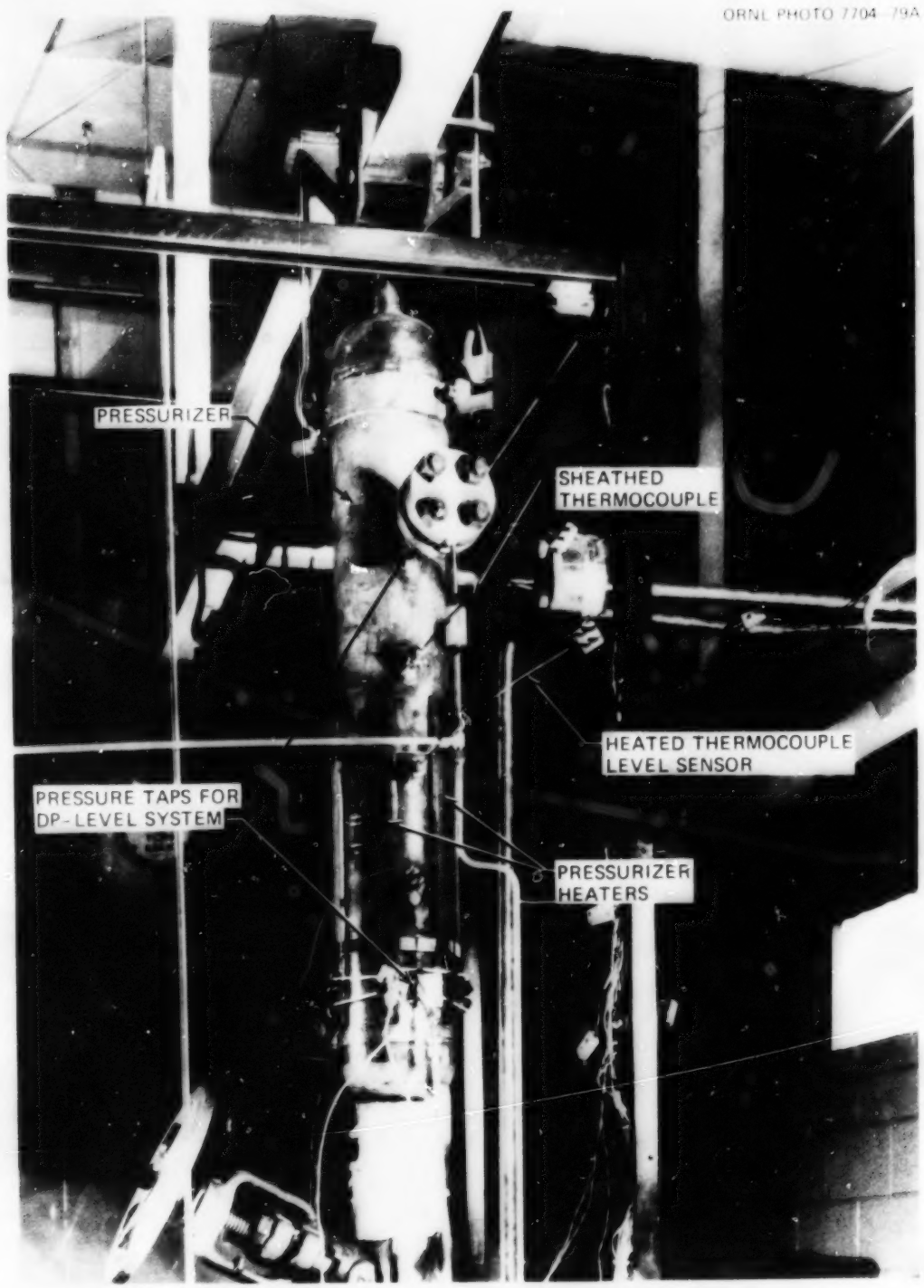

Fig. 1. Photograph of pressurizer in TITF. Installed thermocouple probes are shown near center of photograph. After installation of level sensors, the pressurizer was installed with mineral fiber insulation.

assembly. The sensor assembly was then insulated with a ceramic cement and inserted into a 3-mm-OD capsule, which was then brazed to the end of the lead assembly. Thermocouple and heater leads were terminated with a pair of standard male thermocouple plugs, Chromel-Alumel and Copper-Copper, respectively.

2.1.3 Test description

For the scoping tests of the HTC level sensor, the sensor described above was inserted into the lower of two ports to the pressurizer on the TITF loop. A standard 3-mm-diam sheathed Chromel-Alumel thermocouple was inserted in the upper port, which was located about 15 cm above the lower port. This upper thermocouple served both as a differential thermocouple for the HTC and, separately as a test for applicability of the loop-current-step-response method to determine liquid levels.

In the initial tests, the HTC was connected differentially to the normal upper thermocouple. In this way, as the pressurizer was heated, changes in ambient pressurizer temperature would tend to cancel out. Differential output was attached to a strip chart recorder; output of the upper thermocouple was attached to a high-impedance digital temperature indicator to monitor the pressurizer temperature. A constant current supply was connected to the heater and adjusted to give either 150 or 300 mA. The liquid level in the pressurizer was then raised and lowered, and temperature changes were recorded on the strip chart recorder.

The trace in Fig. 2 was taken from run 10 at 200°C. Run 10 had several features common to all runs in this series. A dip of 5°C occurred as the probe was uncovered, presumably caused by evaporation of the water film remaining on the probe. Temperature of the probe increased to about 8.5°C above ambient and stabilized after about 1 min. Upon raising the water level, the temperature of the probe decreased 13.5°C. The temperature changes did not strictly reproduce upon raising the water level because the pressurizer was cooled by the incoming water as it refilled. This experiment showed, however, that, even with a relatively modest heat input, the HTC probe gave a clear indication of liquid level.

In the second series of tests, an alternative method of operation was chosen: instead of a constant heater current, emf output of the

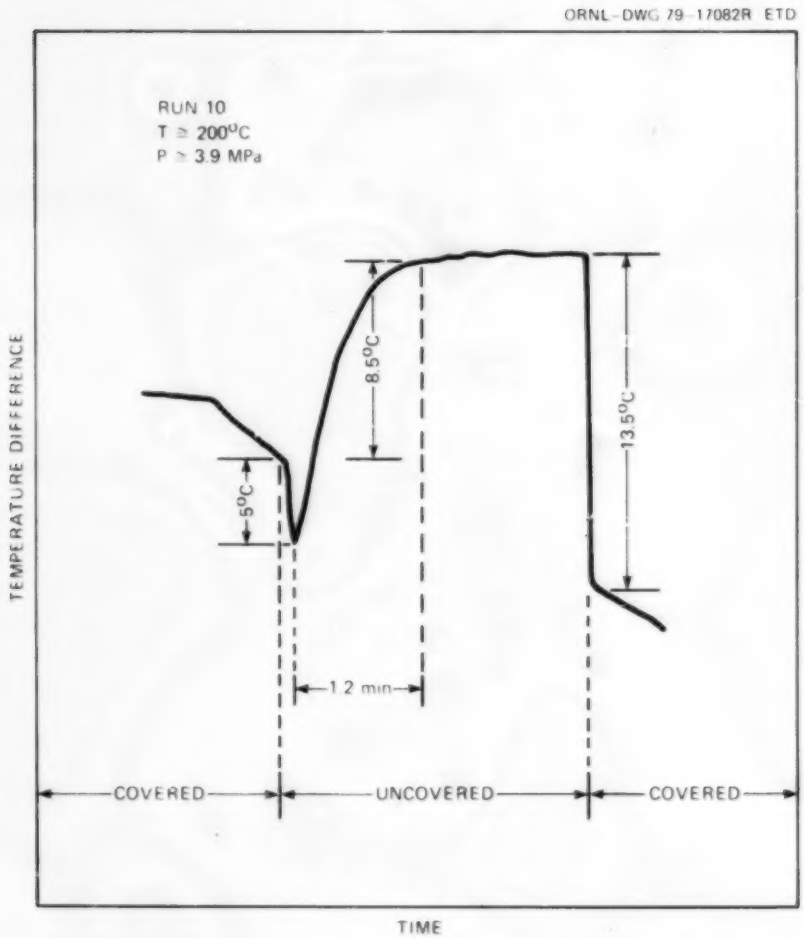

Fig. 2. Experimental results with prototype HTC level detector with constant heater power.

differential thermocouple was connected to a three-mode proportional controller. A two-pen strip chart recorder was used to record both thermocouple output and heater voltage. In this mode of operation, changes in the heater voltage were used to indicate the presence or absence of liquid around the probe. A bJock diagram of the measuring equipment is shown in Fig. 3. Figure 4 shows one run made near room temperature with the HTC in the heater voltage indication mode. Lowering the liquid level below the probe gave a clear 4-V drop in the heater voltage. When the probe was covered again, heater voltage and temperature both returned to their original values.

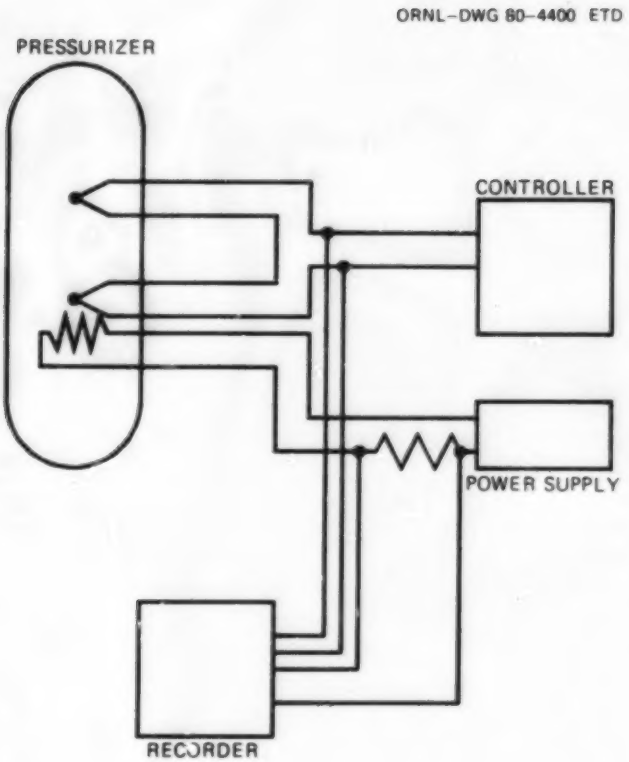

Fig. 3. Block diagram of measurement apparatus used in controlled differential temperature mode.

2.2 Procurement and Fabrication of HTC Sensors

2.2.1 Procurement of naval reactor-type sensors

Personnel of the Naval Reactor Division provided names of current and past suppliers of HTC assemblies used in formerly and currently operating naval reactors. The firm of Robinson-Halpern was contacted; they agreed to make experimental HTC sensors of the Naval type to specification for experimentation. An order was placed for five 3- and five 1.6-mm-OD sensors. Delivery is expected in March 1980.

2.2.2 ORNL fabrication

The fuel rod simulator fabrication group at ORNL completed two 3-mm-OD probes that included both differential thermocouple junctions within

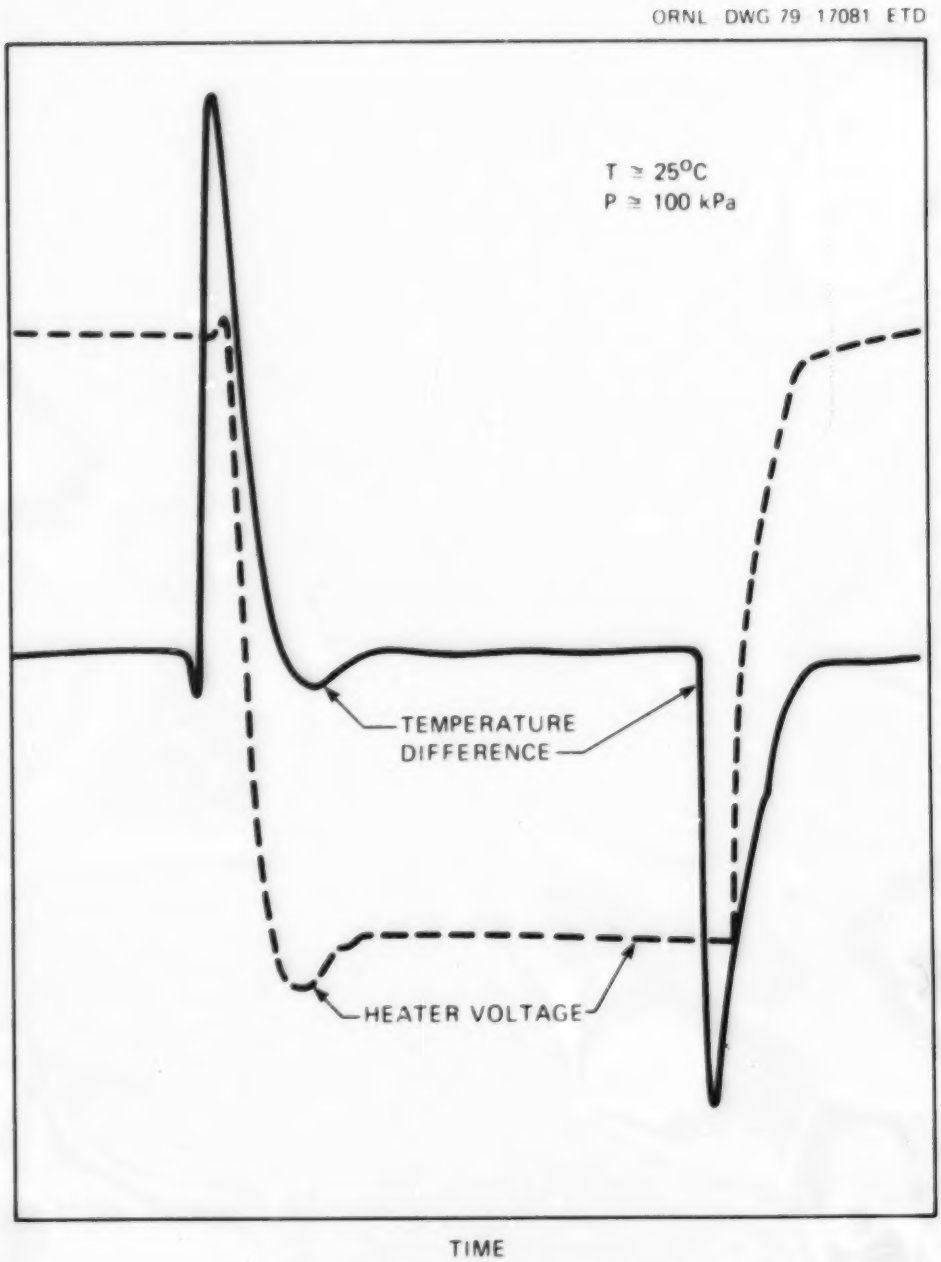

Fig. 4. Test of HTC with proportional controller to maintain constant differential temperature. Solid curve is temperature difference; dashed curve is voltage across heater.

the same sheath. This will substantially reduce the effects of ambient temperature fluctuations on the sensor indication. A schematic design of the sensors and a photograph of one of the sensors during fabrication appear in Fig. 5(a) and (b), respectively. The design reflects improvements suggested by the initial prototype testing: a reference thermocouple is located some 30 mm (1.2 in.) from the end of the heated region but in the same probe assembly as the HTC. (To date, scoping tests have been performed with level probes inserted horizontally; future tests may investigate operation with level probes in vertical orientations.)

Improved sensitivity of the new probes will allow operation of the probe heater at lower temperatures with consequent improvement in reliability and reduced likelihood of occurrence of metal-water reactions. Tests are being planned to establish optimum operating parameters so that unambiguous readings will result under all possible fluid conditions.

2.3 Loop-Current-Step-Response Tests

The loop-current-step-response apparatus was developed at ORNL for in situ testing of installed thermocouples, for example, in a nuclear reactor. Because the time response of a thermocouple sensor is strongly influenced by the heat conduction of the surrounding medium, a series of tests were run with the loop-current-step-response apparatus to determine if the method would be suitable for in-core liquid level detection using the available core thermocouples.

In the loop-current-step-response method, a current is passed through the thermocouple wires with a consequent temperature rise of several degrees centigrade. Decay of this temperature is recorded when the heating current is turned off. The time constant of the sensor can be determined from the shape of the temperature decay curves and is directly related to the thermal conduction between the sensor and its surroundings. When the sensor is immersed in liquid with relatively high thermal conductivity, decay of temperature is more rapid than when it is immersed in vapor with only a fraction of the thermal conductivity of the liquid. Some results of these tests are shown in the oscillographs in Fig. 6.

ORNL–DWG 80–4401 ETD

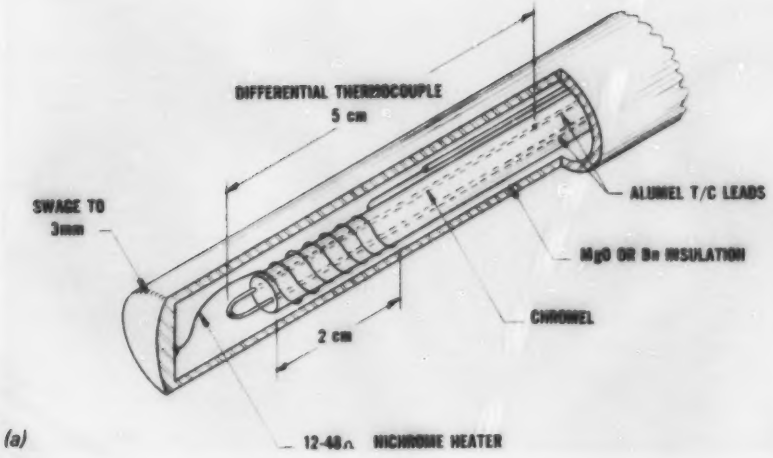

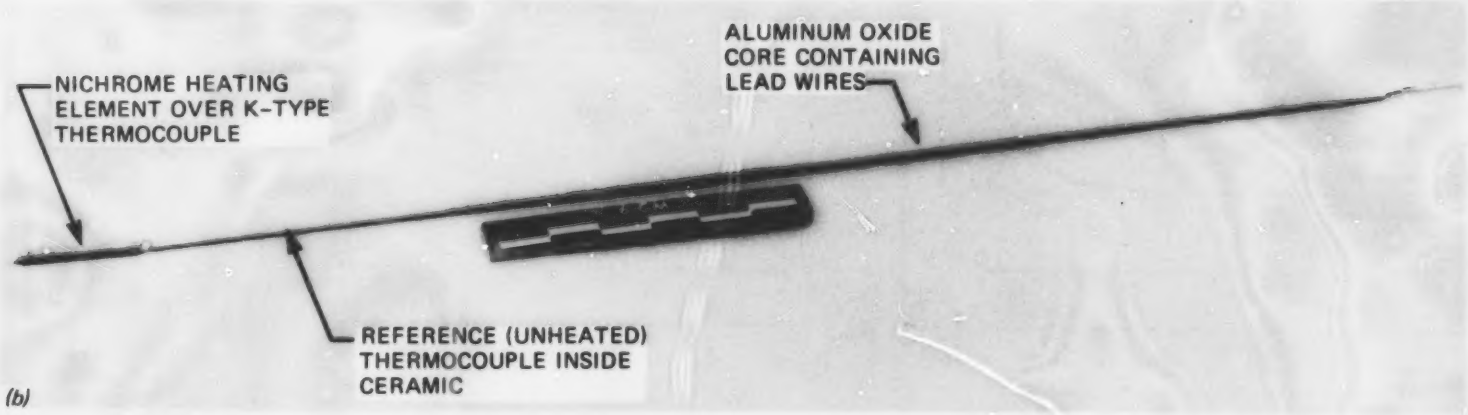

Fig. 5. Drawing of new prototype differential thermocouple liquid level probe (a) and photograph of internal heater and thermocouple assembly (b).

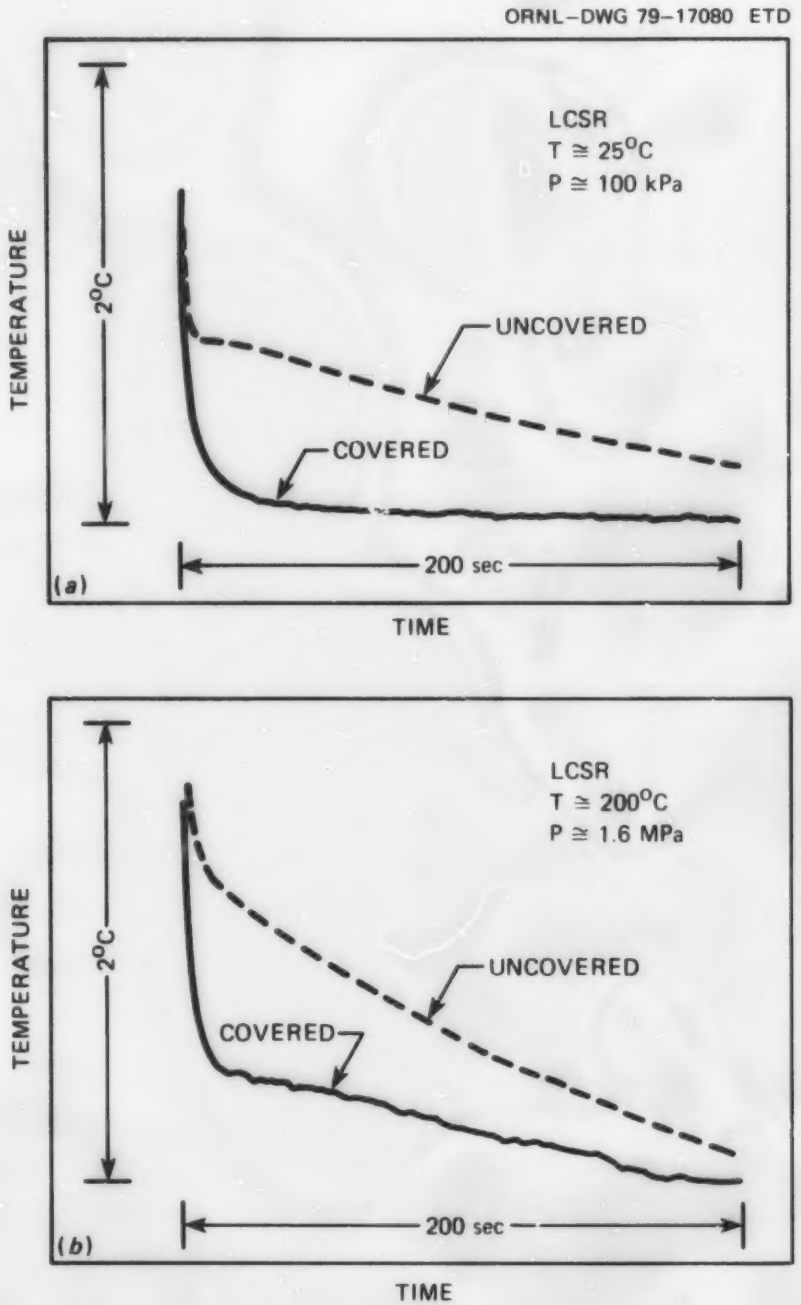

Fig. 6. Oscillographs obtained from loop-current-step-response test in TITF of a normal 3-mm-diam thermocouple as a liquid level sensor. For all traces, full-scale temperature (vertical) axis is approximately 2°C; full-scale time (horizontal) axis is 200 s. (a) Data recorded at room temperature; (b) data recorded at 200°C.

At room temperature and pressure [Fig. 6(a)], a clearly discernible difference was seen between the time response of the liquid-covered probe and the probe immersed in vapor. At 200°C [Fig. 6(b)] the difference between the time response of the two probes was not as great but was clearly detectable. Restrictions of the power supply in the present loop-current-step-response apparatus limited the temperature rise in the 3-mm-diam thermocouple to about 2°C.

2.4 THTF Fluid Thermocouple Signal Analysis

An analogue data acquisition system was used to record millivolt signals from thermocouples used for measuring fluid temperature in the test section of the THTF during the first series of bundle boiloff experiments. Data recorded are suitable for signal analysis using various techniques. Preliminary studies of the data are in progress.

2.5 Thermal-Hydraulic Model of HTC Level Test

Radial heat conduction modeling of the HTC has been carried out using a RELAP4 computer model of the TITF pressurizer and HTC sensors to aid in understanding (1) thermal-hydraulic response of the pressurizer during filling and draining operations, (2) heat transfer characteristics of steam and water at various temperatures and pressures and with very low flow rates, and (3) transient response of heated and reference thermocouples inside the sensor probes. Proposed sensor design improvements and testing methods may also be scoped using the computer model.

2.6 Ultrasonic Method

An ultrasonic probe using the torsional mode of propagation for measuring liquid level is being evaluated for accuracy and repeatability in a level test facility at ORNL. The sensor itself is simply a 3-m-long flattened stainless steel ribbon, excited in a twisting mode by a circularly magnetized magnetostrictive rod attached to the end of the ribbon. Propagation velocity in the sensor is dependent on temperature and density of the surrounding medium. The sensor is divided into zones; reflections

from different zones serve to indicate the density of the surrounding fluid.

Using the ultrasonic sensor at ambient conditions with laboratory variation in temperature of 10°C or less, uncertainty in the water level was ±4%. Under steady temperature conditions, uncertainty in the measured level was ±0.5%. The intent now is to measure temperature concurrently and compensate the level indication.

2.7 Contacts with Utilities and Reactor Vendors

In December, ATPI program staff members met with members of the nuclear power plant design group of TVA in Knoxville. The purpose of the meeting was to inform TVA of progress in the development of level detection devices and to obtain information about installation and use of reactor vessel instrumentation. Subsequently, a visit was made to TVA Watts Bar Nuclear Plant Site to see components of the reactor instrumentation system and to hold discussions with TVA on-site personnel.

Directing research so that hardware and methods developed may be applied in operating and planned power reactors is desirable. For this purpose several telephone conversations were held with persons associated with the development of in-vessel level detection systems for reactor vendors.

3. SIGNAL ANALYSIS STUDIES WITH DRAG FLOWMETERS

C. E. Davis*

A third test of drag target cross-correlation for use as a transit-time flowmeter has been completed in the Air-Water Test Facilty (AWTF). Two Ramapo drag flowmeters, separated by a distance of 62.2 cm (24.5 in.), were tested in two-phase air-water vertical upflow. Using signal analysis in the frequency and time domains, the transit times of flow disturbances between the two sensors and the implied velocities were determined.

3.1 Methods

Design and operation of the ORNL AWTF are described in a previous quarterly report.[3] Advanced Spool Piece I, installed for vertical upflow in the AWTF (Fig. 7), was used for the drag flowmeter tests with instrument separation of 62 cm. Four air flow rates ranging from 2.2 to 34 g/s (4 to 64 scfm) were used; water flow rates ranged from 2.5 to 18.9 liters/s (40 to 300 gpm).

On-line cross-correlation of the two drag flowmeter signals was performed with a Hewlett-Packard 5420A signal analyzer. The transfer function in the frequency domain was the primary signal analysis method; however, certain flow conditions were also examined in the time domain using the cross-correlation function.

For frequency domain analysis, the mean velocity of flow disturbances between the two instruments is calculated as

$$V = \frac{360\ D}{\theta'} , \qquad (1)$$

where D is separation distance between the two instrument sensors and θ' (degrees/Hz) is slope of the phase shift curve. In the time domain, mean transient time between sensors was the time at which a maximum in the cross-correlation function occurred.

---

*Engineering Technology Division.

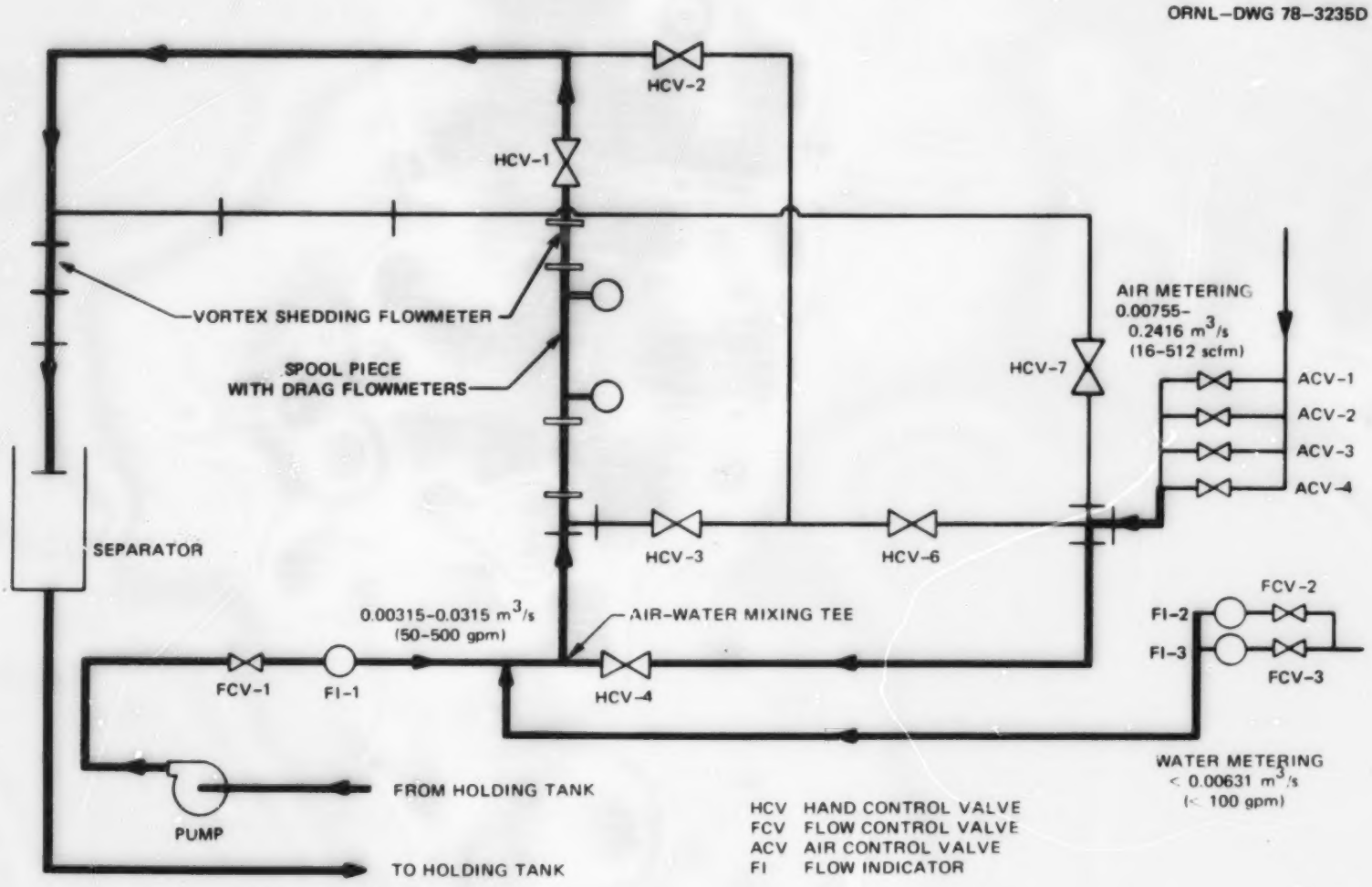

Fig. 7. Schematic of Air-Water Test Facility showing locations used for testing vortex and drag flowmeters.

Experimental transit time flowmeter (TTF) tests used large "full flow" drag bodies of the bladed type with two Ramapo Model Mark V drag flowmeters in 8.9-cm-ID (3.5-in.) pipe. The test condition of each run included the slug-flow and bubble regimes which are depicted on the vertical upflow flow regime map of Oshinowo and Charles.[4] Void fraction for each flow condition (obtained for the three-beam gamma densitometer) was then used to calculate time- and space-averaged liquid and gas velocities according to the separated-flow model.[5]

3.2 Results

The third drag target transit-time flowmeter test resulted in 17 data points (Table 1). (The first two tests, described in a previous report,[6] involved drag target separations of 15 and 29 cm, respectively.) During this third test, a wide spectrum of conditions within the slug-flow regime was obtained.

The calculated transit-time velocities compare well with previous studies of drag flowmeters at different separation distances. At low air flow rates, indicated transit-time velocities are less than velocities obtained at the same flow rates with a shorter separation distance; however, at air flow rates greater than 2.2 g/s the indicated velocity is either equal to or greater than that obtained with a shorter separation distance. Experimental data (Fig 8.) indicate that there was a significant loss of coherence between the drag flowmeter signals as the separation distance was increased. This is a possible cause of the variation of the indicated transit-time velocities (usually <10%) between the runs with different separation distances. Poorer coherence leads to larger errors in the estimation of the slope of the phase-shift curves and in the estimation of the velocities. Low coherence was present during the entire test with the 62-cm separation distance. Plots of the coherence function (Fig. 8) indicate that, from the sensors, the majority of the signal that was correlatable in the frequency domain was low frequency (<10 Hz). Occasionally, good coherence was observed up to 35 Hz; this was normally seen during exceptionally strong slug pulses.

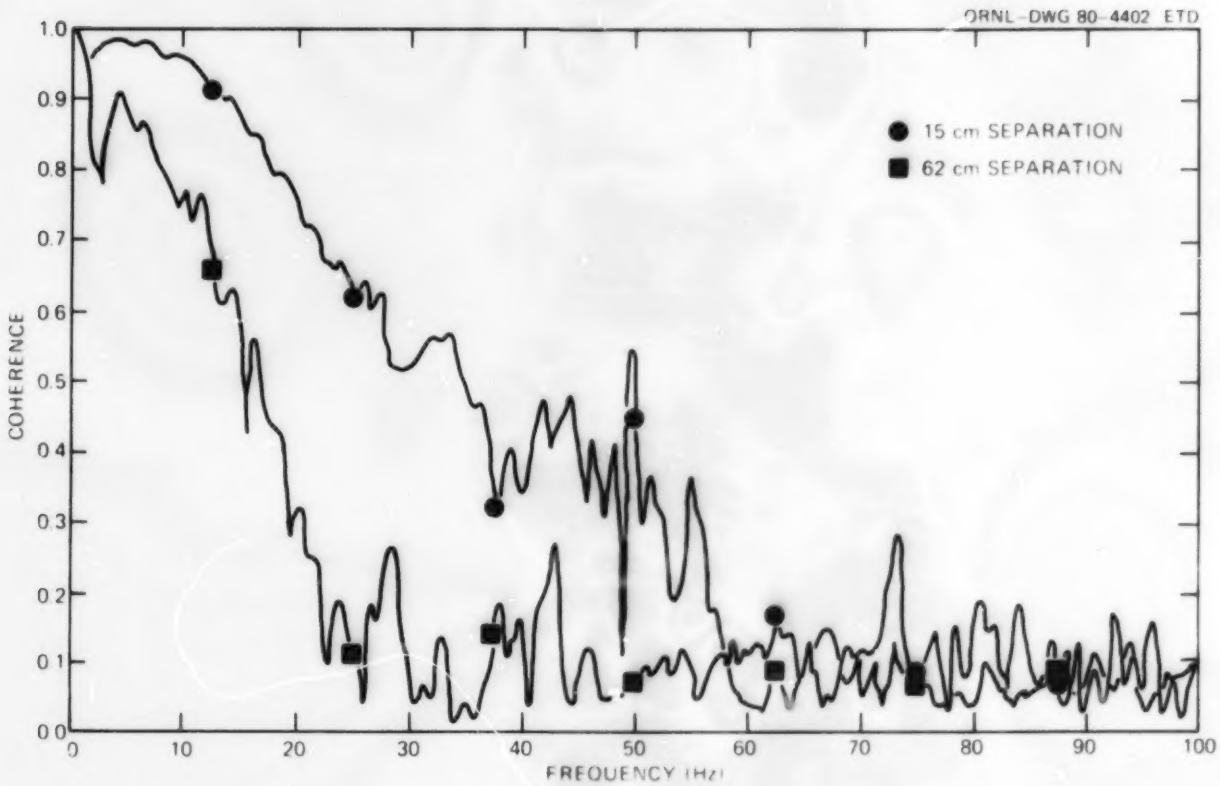

Fig. 8. Coherence of signals from two drag flowmeters in two-phase vertical upflow with superficial water and air velocities equal to 2.0 and 1.2 m/s, respectively.

Table 1. Drag target transit-time velocity results with a sensor separation of 62.2 cm

Superficial velocity (m/s)		Phase velocity[a] (m/s)		Transit-time velocity (m/s)		Flow regime[b]
Water	Air	V_f	V_g	Frequency domain	Time domain	
0.4	0.3	0.5	1.5	2.5	1.8	Quiet slug
0.6	0.3	0.7	1.7	2.5	2.3	Quiet slug
1.0	0.3	1.2	2.2	3.1		Quiet slug
2.0	0.3	2.2	3.8	4.5		Bubble
3.0	0.3	3.2	7.0	4.9		Bubble
0.4	0.6	0.6	1.9	2.3	2.6	Quiet slug
0.6	0.6	0.9	2.1	2.7	2.6	Quiet slug
1.0	0.6	1.3	2.5	2.7	3.0	Quiet slug
1.5	0.6	1.9	2.9	3.6	3.4	Quiet slug
0.4	1.2	0.8	2.4	3.1		Dispersed slug
0.6	1.2	1.1	2.9	3.4		Dispersed slug
1.0	1.2	1.8	2.9	3.6	4.1	Dispersed slug
2.0	1.2	2.8	4.1	4.5	4.8	Dispersed slug
0.4	4.9	1.5	6.7	5.2		Frothy slug
0.6	4.9	2.0	7.0	5.2	5.4	Frothy slug
1.0	4.9	2.9	7.5	6.0		Frothy slug
2.0	4.9	4.1	9.6	7.8	7.8	Frothy slug

[a] Phase velocity based on the separated flow model.[5]

[b] Based on flow regime map of Oshinowo and Charles.[4]

Drag flowmeter signals were also analyzed in the time domain with the cross-correlation function. A definite peak occurred in the cross-correlation function, indicating a mean transit time of flow disturbances between sensors. Velocities calculated from these transit times compare well with those velocities calculated from the phase-shift curve in the frequency domain for each flow condition. Study using the drag flowmeters as transit-time flowmeters is continuing.

4. VORTEX SHEDDING FLOWMETER

This section describes an experimental study done at ORNL to examine the utility of a commercially available vortex shedding flowmeter for making velocity measurements in two-phase flow. Vortex flowmeters are attractive for this application because they are rugged, have no moving parts exposed to the flow, and are relatively insensitive to long-term variations in fluid density and viscosity. Vortex flowmeters might be expected to succeed in a postulated homogeneous one-dimensional two-phase flow field. However, actual inhomogeneities in the flow tend to disperse the vortices shed by the bluff body or to redirect them so they do not interact with the vortex-sensing transducer in a consistent manner. In the ORNL AWTF, a commercially available vortex shedding flowmeter (Fischer and Porter Company Model 10LV) was tested in two-phase flow to study the severity of this problem.

Initial studies made with a vortex shedding flowmeter in two-phase vertical downflow were described previously.[7] Subsequent experiments have involved tests of the flowmeter in upflow and the use of a digital signal analyzer for data processing. Strouhal described the basic characteristics of the wake (Fig. 9), which is also known as the Karman vortex trail or street. Strouhal found that the frequency of vortex formation f was directly proportional to the fluid speed V and inversely proportional to the diameter of the bluff body d:

$$f = K(v/d) . \qquad (2)$$

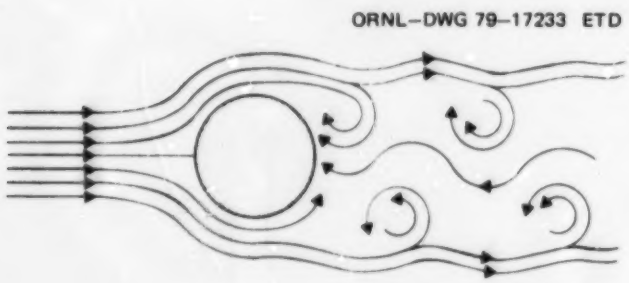

Fig. 9. Karman vortex street pattern behind right circular cylinder.

The proportionality constant K is known as the Strouhal number. For a circular cylinder, the value of the Strouhal number is essentially constant at 0.20 over a Reynolds number range of 2,000 to 100,000. When the shedding body is enclosed in a conduit carrying fluid, there is some effect of conduit size on the vortex shedding frequency; however, even then, the Strouhal number is constant for a wide range of flow rates. In a homogeneous flow stream, because there is no effect of fluid density or viscosity on the vortex shedding frequency, the attractiveness of vortex shedding as a measurement scheme in dispersed two-phase flow is shown. (Other commonly used velocity meters such as turbines or Pitot tubes do exhibit a dependence on density or void fraction.)

4.1 Description of Test Meter

The bluff body in the test meter (Fig. 10) consisted of a compound shape designed to enhance the amplitude of pressure fluctuations due to the passage of vortices. A single strain-gauge sensor is embedded in the body to sense forces along the vectors AB in the plane of the paper in Fig. 10. Net strain resulting from all forces on the downstream portion of the body is sensed. Thus, the average of flow forces that are normal to the body, rather than localized effects, are detected. This design was judged to have a greater probability of success than designs with a single shedding body and a localized vortex-sensing transducer. Because of recent advances in strain-gauge technology, meters of this design

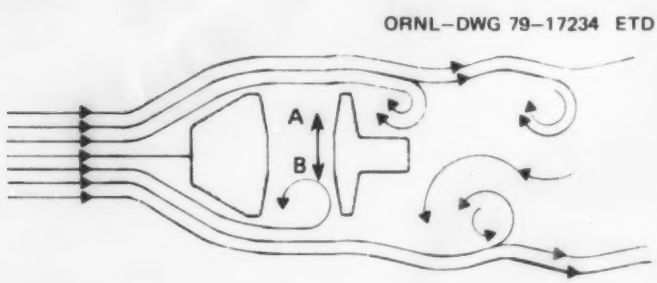

Fig. 10. Vortex street pattern generated by compound bluff body in vortex flowmeter. Force variations along AB are detected by strain gauge.

probably could be adapted for operation at high temperatures typical of some loss-of-coolant-accident (LOCA) experiments.

The flow element (shedding body) in the test meter is mounted transversely in a flanged flow tube (Fig. 11). The tube is inserted into the downstream pipe, and the flange ring fits between the two adjacent piping flanges. A signal conditioning module is mounted on the flanged part of the meter.

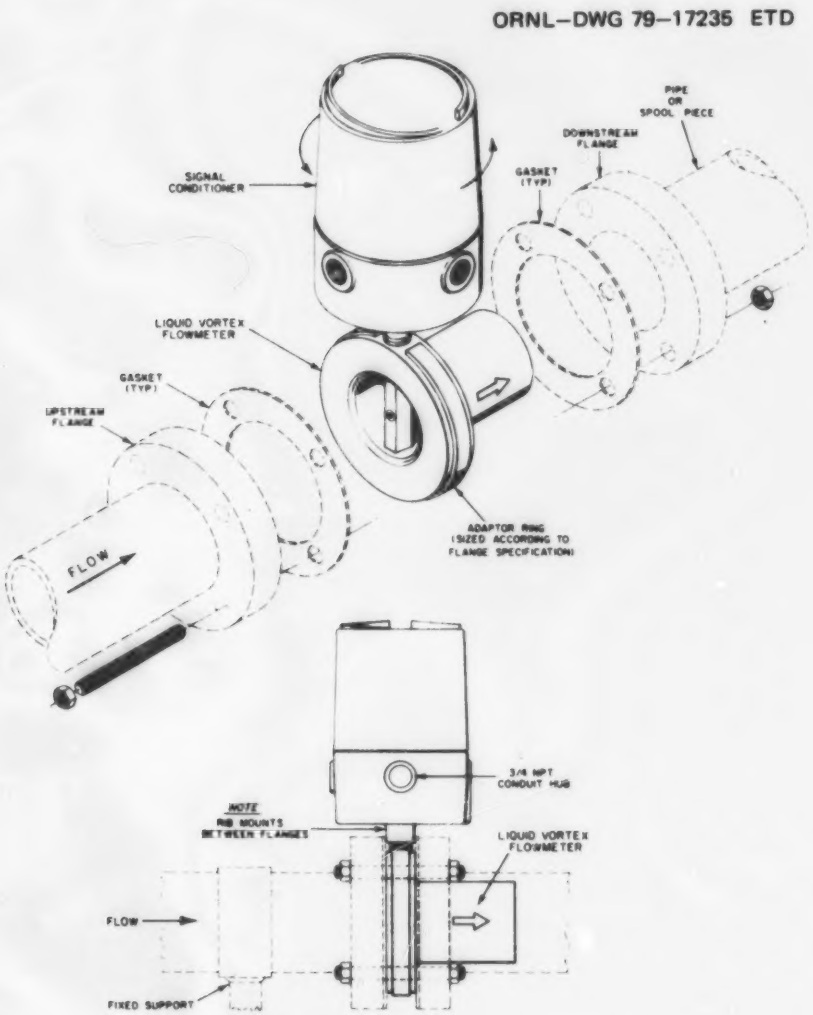

Fig. 11. Installation details for vortex flowmeter.

4.2 Test Methods

The test meter was installed in the AWTF in two positions indicated in Fig. 7. To observe the two-phase flow regimes occurring in the system, the AWTF consists primarily of transparent 4-in. nominal polyvinyl chloride (PVC) pipe. The position for vertical downflow testing was 1.4 m (4.5 ft) from the elbow leading to the downcomer and 1.1 m (3.5 ft) above the flow separator. For vertical upflow testing, the meter was installed 2.2 m (7.2 ft) above the tee leading to the riser and 1.1 m (3.5 ft) below the tee connecting to the horizontal run of pipe at the top of the loop. According to operating instructions supplied by the manufacturer, inclusion of a straight length of piping equivalent to ten pipe diameters (1.0 m in this case) is recommended for optimum meter performance.

In the AWTF, critical flow orifices are used for metering air flow, and rotameters and magnetic flowmeters are used for water metering. Air flow rates ranging from 0.6 to 288 g/s (1 to 512 scfm) and water flow rates from 0.3 to 32 liters/s (5 to 512 gpm) were used for the vortex meter testing. Superficial velocities in the test section ranged from 0.07 to 40 m/s (0.25 to 128 fps) for air and 0.05 to 5 m/s (0.2 to 17 fps) for water. The useful flow range of the meter was 2.5 to 39 liters/s (40 to 600 gpm).

Because many other possible flow rate combinations were found to produce meaningless signals from the test meter, flow rate combinations yielding high or low void fractions were considered primarily. Mixing of air and water occurred in the vicinity of a divider plate installed at the tee shown in Fig. 7. During two-phase operation in the AWTF, temperatures were ~25°C (77°F) and pressures were >360 kPa (51 psia).

The signal-conditioning electronics supplied with the vortex flowmeter serve to amplify and shape the process variable-frequency signal, to improve the signal-to-noise ratio, and to convert the frequency to a 4- to 20-mA analogue current proportional to the vortex shedding frequency. Electronic components used in the AWTF experiments are shown schematically in Fig. 12. In these tests, current meters and chart recorders were used to record the analogue output signal from the signal conditioner unit. In addition, output of the strain-gauge sensor within

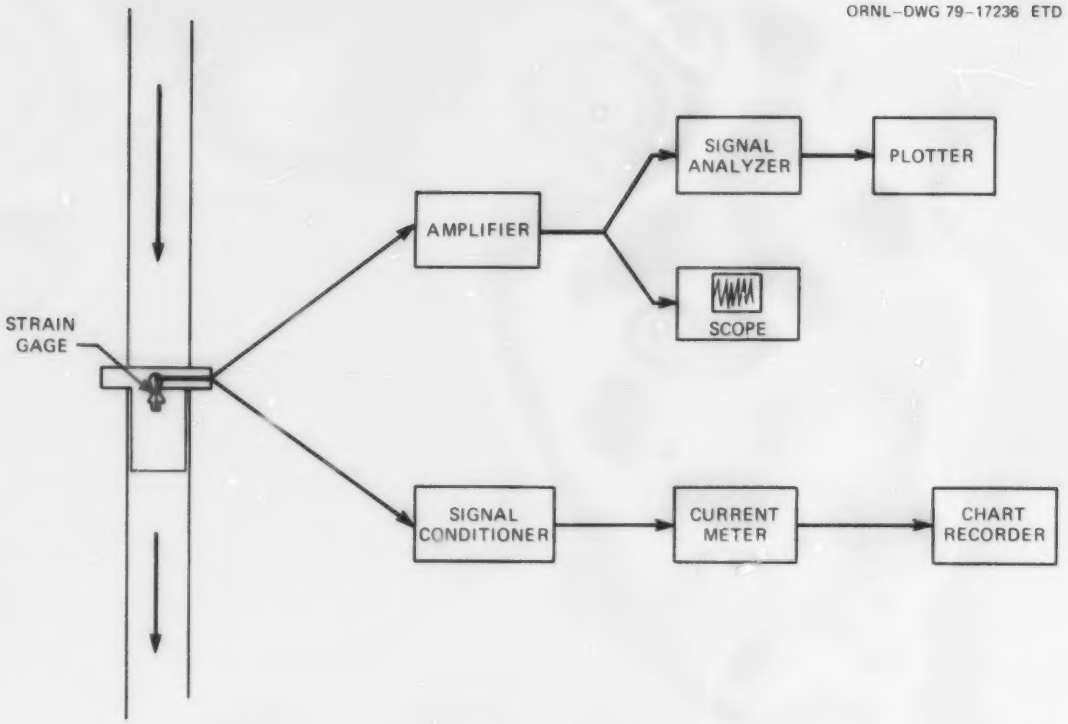

Fig. 12. Block diagram of electronics used for vortex flowmeter testing.

the flow element was monitored directly by means of a terminal strip in the signal-conditioning module. Outputs from the strain gauge were ac coupled and amplified using a Princeton Applied Research Model 113 amplifier. Amplifier output was routed to a storage oscilloscope where time traces were photographed. In some tests, a digital signal analyzer was used to perform on-line analysis of the strain-gauge signals. The signal analyzer performs a Fourier transform on the input signal so that parameters such as the signal power spectrum may be displayed in the frequency domain. Long averaging times (e.g., 100 s) were used so that good statistical averages of the signal behavior were obtained.

4.3 Results

Single-phase and two-phase tests were performed in both upflow and downflow.

4.3.1 Single-phase flow

The test flowmeter performed satisfactorily in all-water flow in both orientations. (The meter is marketed specifically for liquid flow service.) Analogue output of the signal conditioner converted to flow rates which agreed with those from the magnetic flowmeter within a few percent. Figure 13 shows the output of the strain-gauge transducer vs time for all-water flow rates of 6.25, 15.6, and 25 liters/s (100, 250, and 400 gpm).

Obtaining velocity measurements in single-phase air flow was also possible, but pressure oscillations on the flow element caused by vortex shedding created signals that were too small to trigger the signal conditioner counting circuit threshold. For air flow, well-defined low-amplitude waves were visible on the oscilloscope (Fig. 14). These signals were processed with the signal analyzer, yielding the power spectrum vs frequency plot shown in Fig. 15. However, with air input rates below about 69 g/s (128 scfm) or air velocities below about 10 m/s, the signals could not be distinguished from background noise.

4.3.2 Two-phase flow

In two-phase flow, the vortex flowmeter was found to yield information about flow field velocity at very low and very high void fractions. The range of void fractions for which the meter worked was somewhat wider when the velocity in the pipe was high.

With high water input rates, output from the signal-conditioning electronics that were provided with the meter was oscillatory and indicated progressively lower flow rates as more air was introduced. The meaning of those signals was not interpreted. Behavior of the output signal from the flow element strain gauge as void fraction was increased (air was added to an initially all-water stream) is illustrated by the oscillographs in Fig. 16. For all frames, the water flow was downward at 19 liters/s (300 gpm). Successive frames show the output signal at 0, 1.1, 2.2, and 4.5 g/s (0, 2, 4, and 8 scfm). Data taken at almost the same location in the system using a three-beam gamma densitometer indicate that the air volume fraction or void fraction for these flow rates was approximately 0, 0.033,

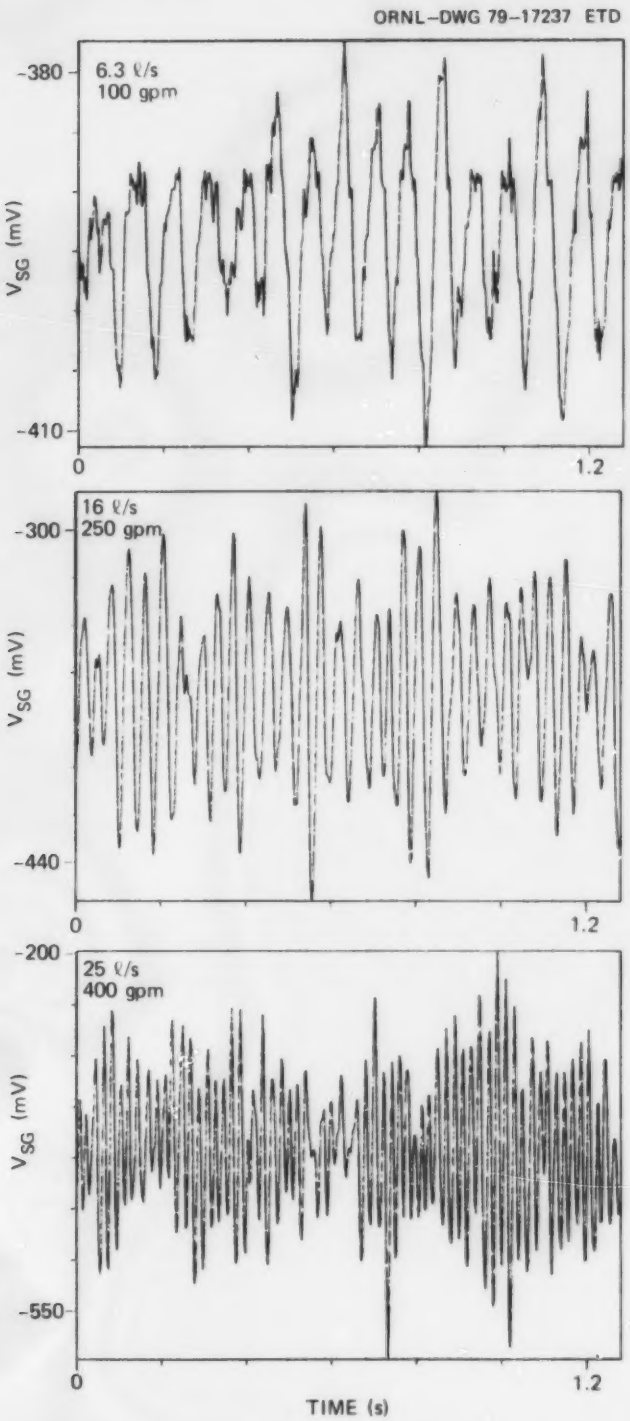

Fig. 13. Output of flowmeter strain gauge vs time for three single-phase water flow rates. Full-scale ordinate is different for each graph.

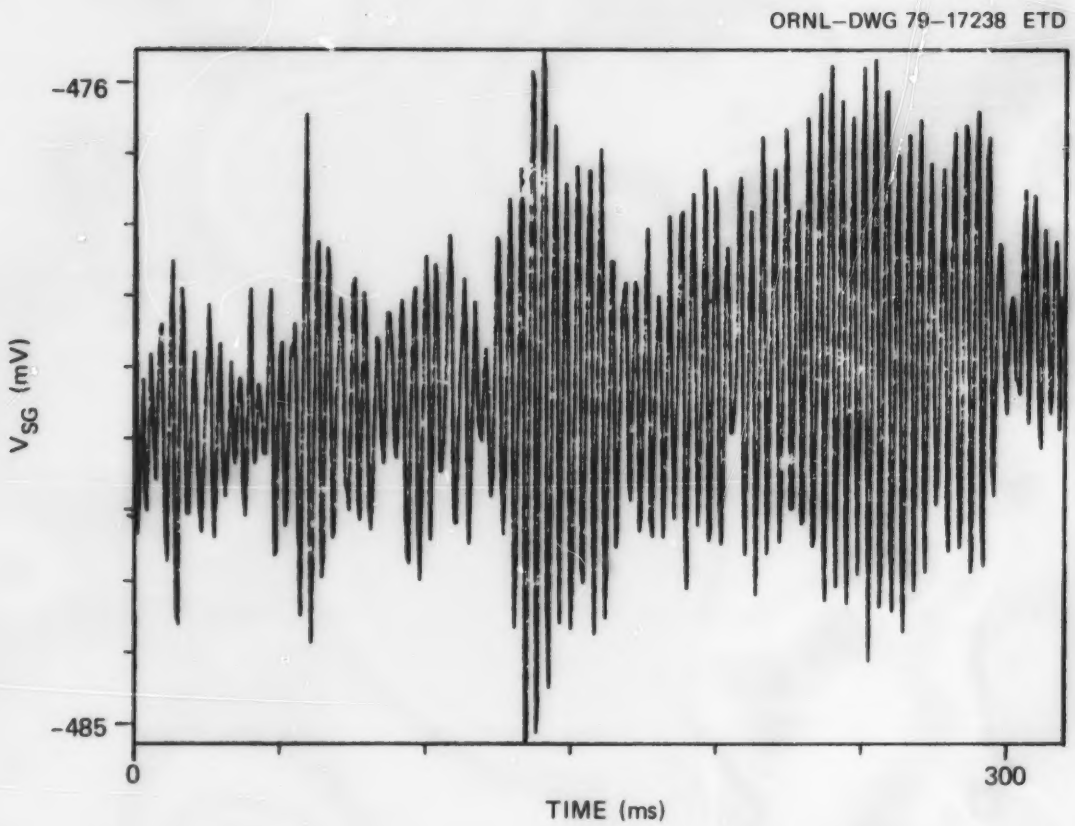

Fig. 14. Output of flowmeter strain gauge vs time for single-phase air flow at 216 g/s (384 scfm).

0.07, and 0.17, respectively. The flow regime observed was bubbly flow. As can be seen (Fig. 16.), the signal fluctuations due to vortex shedding from the flow element deteriorated with increasing void fraction. When the vortex shedding oscillations were occurring, their magnitude was not greatly reduced compared with their magnitudes in single-phase water flow. However, periods when the vortex signal was occurring became shorter and less frequent with higher air flow rates. Signals observed at other times are believed to be flow noise or 60-Hz noise.

A digital signal analyzer was used to provide information on the frequency content of the signal from the vortex meter under various flow conditions. Analysis of the signals obtained at 25 liters/s water flow (400 gpm) with air flow rates of 1.1, 2.2, 3.3, and 4.5 g/s (2, 4, 6, and 8 scfm) led to the power spectrum plots shown in Fig. 17. With increasing

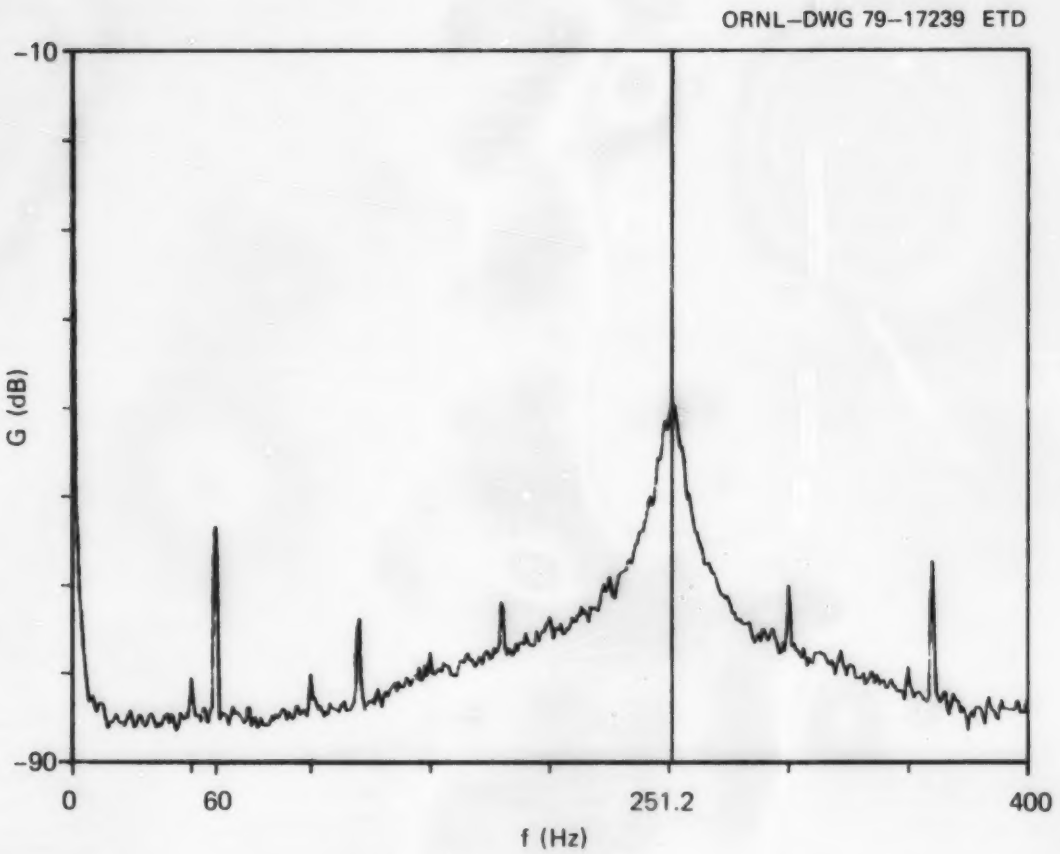

Fig. 15. Power spectral density of signal from flowmeter with single-phase air flow of 216 g/s (384 scfm).

air flow rate, the predominant frequency content of the signals becomes broadened and the total signal power decreases. To get indications of the approximate velocity under two-phase conditions, the peak channel in the power spectral density can be observed. When that method was used, velocities which were indicated by the meter in low-void-fraction two-phase flow increased with increasing air flow (Fig. 17). This is to be expected because, with constant volumetric flow rate of water, introduction of air leaves less flow area to be occupied by the water; thus, higher mean velocities will occur.

Similar behavior of the vortex meter was observed when small quantities of liquid were introduced to high-speed air flows. Figure 18 shows

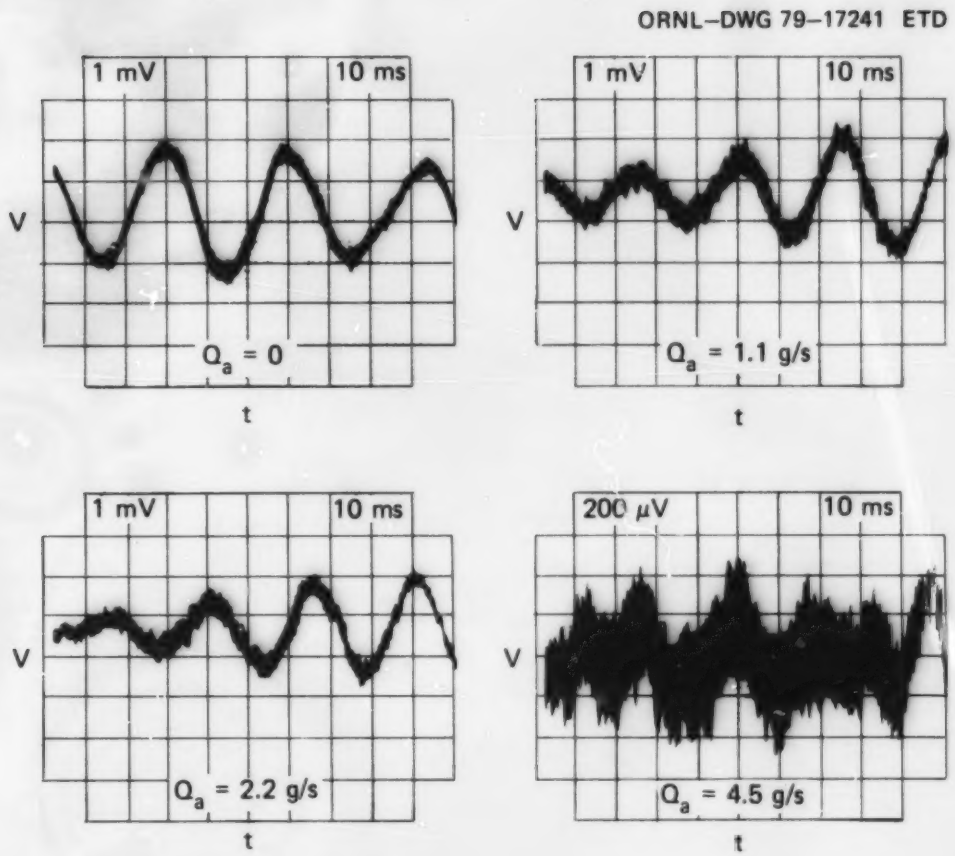

Fig. 16. Output of flowmeter strain gauge vs time for 19 liters/s (300 gpm) water flow and 0, 1.1, 2.2, and 4.5 g/s (0, 2, 4, and 8 scfm) air flow. Scale units are shown on oscillographs.

oscillographs obtained with 108 g/s (192 scfm) air flow and 0 and 0.063 liter/s (0 and 1 gpm) water flow. For high-void-fraction runs, the vortex signals were generally of higher frequency and lower amplitude compared with the low-void-fraction data shown previously. Power spectral densities at 288 g/s (512 scfm) air flow and 0, 0.3, and 0.6 liter/s (0, 5, and 10 gpm) water flow (Fig. 19) dramatically illustrate the loss of the vortex signal as liquid content increased. The well-defined peak at 450 Hz broadened and virtually disappeared at 0.6 liter/s.

A number of air-water flow rate combinations that produced intermediate void fractions were investigated. Flow regimes were frothy and slug

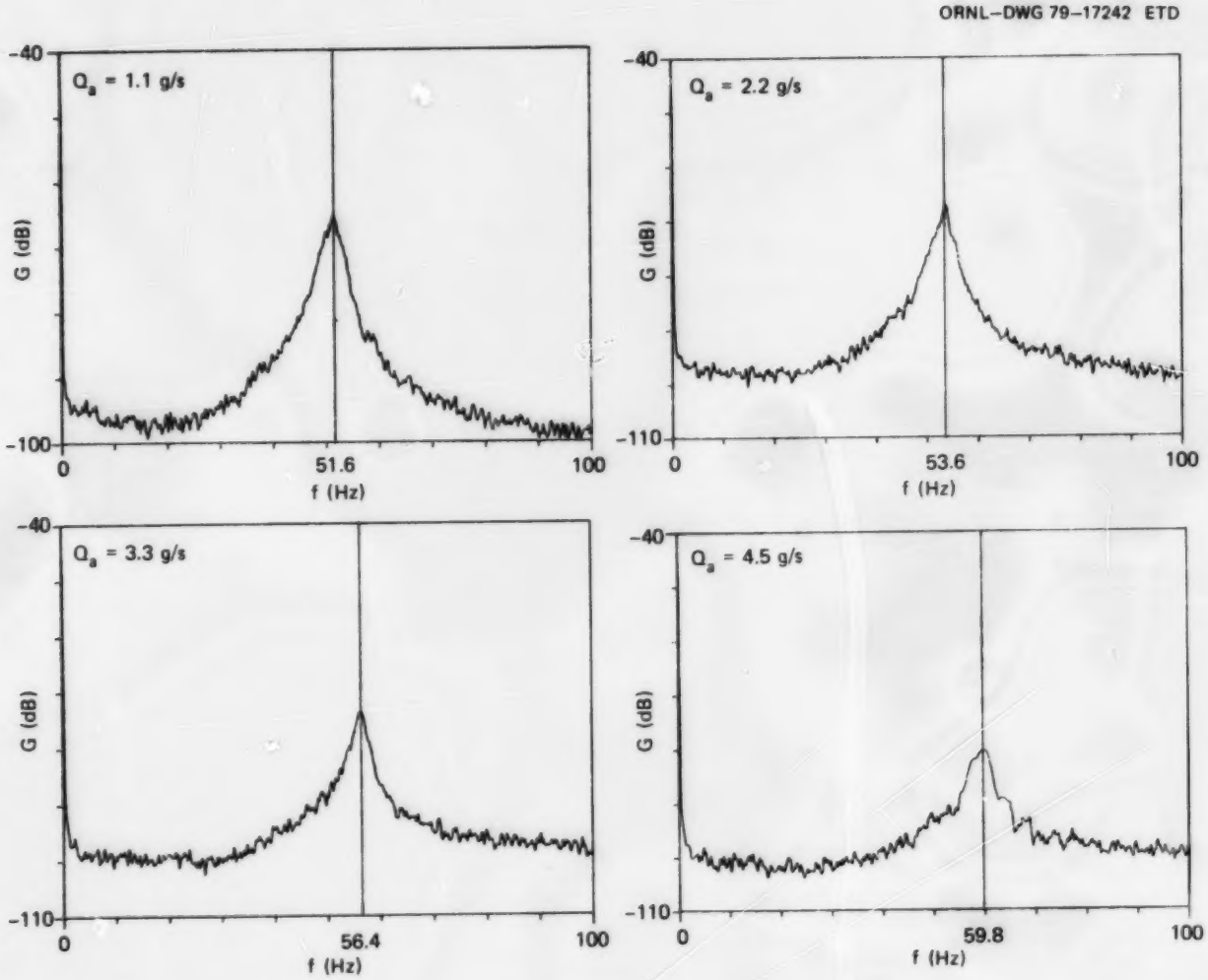

Fig. 17. Power spectral density of signal from flowmeter for 25 liters/s (400 gpm) water flow and 1.1, 2.2, 3.3, and 4.5 g/s (2, 4, 6, and 8 scfm) air flow.

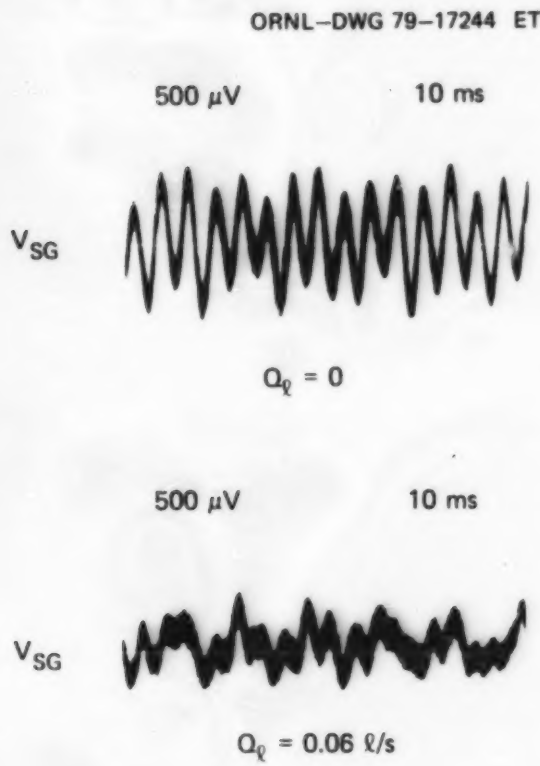

Fig. 18. Output of flowmeter strain gauge vs time for 108 g/s (192 scfm) air flow and 0 and 0.06 liter/s (0 and 1 gpm) water flow. For both oscillographs, full-scale abscissa is 100 ms and full-scale ordinate is 5 mV.

flow. In all cases, no coherent or meaningful vortex shedding signals were obtained with the intermediate void fractions.

There also was little difference between the observations made in vertical upflow and vertical downflow. Data shown in Fig. 17 were from vertical downflow runs; Fig. 20 shows data with approximately the same flow rates from vertical upflow. Due to gravitational effects, a given flow rate of air and water will produce a higher void fraction in downflow than in upflow. Figure 20 shows that the vortex signal fades completely above 4% void fraction in upflow. With high void fraction flows, there was also little difference in the meter's performance between upflow and downflow.

A flow disperser consisting of four stacked layers of 20-mesh/in. screen was placed upstream of the vortex flowmeter when it was installed

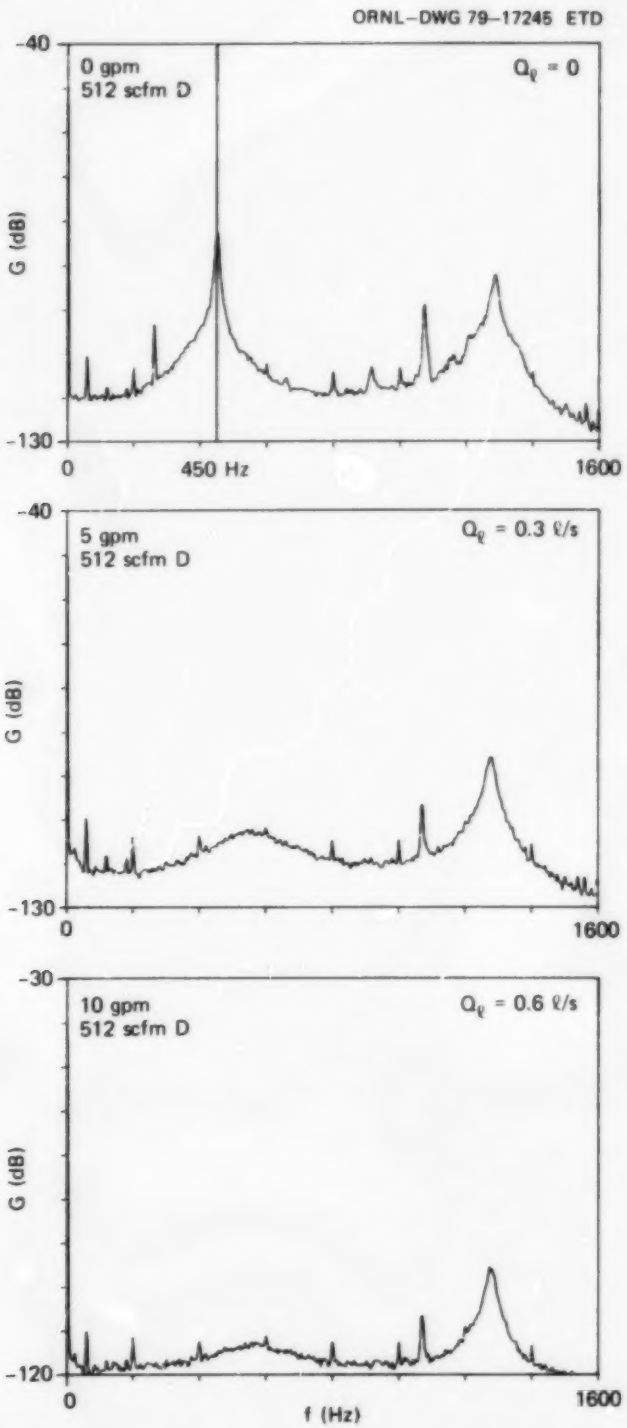

Fig. 19. Power spectral density of signal from flowmeter for 288 g/s (512 scfm) air flow and 0, 0.3, and 0.6 liter/s (0, 5, and 10 gpm) water flow.

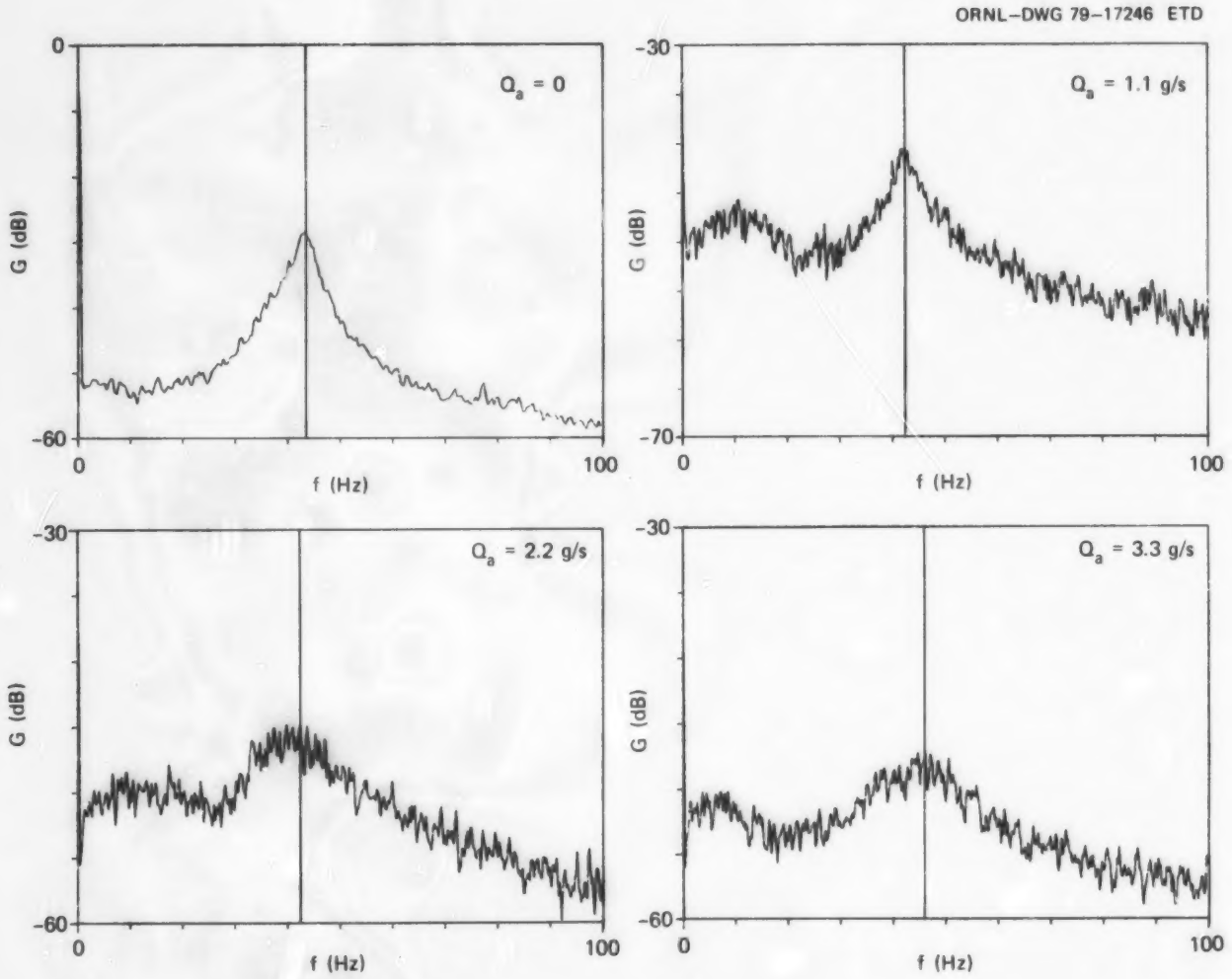

Fig. 20. Power spectral density of signal from flowmeter with two-phase vertical upflow. Water flow rate was 25 liters/s (400 gpm); air flow rates were 0, 1.1, 2.2, and 3.3 g/s (0, 2, 4, and 6 scfm).

for vertical downflow testing. There was no discernable improvement of the signal from the meter in two-phase flow when the flow disperser was used.

4.4 Vortex Flowmeter Summary and Recommendations

Experiments performed in two-phase air-water flow indicate that the usefulness of the vortex shedding mechanism is severely limited for two-phase flow application. The meter tested is generally representative of all vortex flowmeters. Work here at ORNL indicates that vortex shedding can be used to produce clear, modulated signals in a generally homogeneous stream with relatively small quantities of a dispersed phase. Whether vortex shedding simply did not occur at intermediate void fractions or whether vortices were produced but were not sensed because they were obscured by flow noise (generally random pressure variations in the stream) was not determined.

Further research and development of the design of the shedding body, vortex-sensing techniques, and/or signal conditioning probably would not significantly improve meter performance in the intermediate-void-fraction range. Vortex shedding techniques may have some utility for two-phase flow applications at very low and very high void fractions. However, most single-phase flow measurement techniques also work fairly well under those conditions. In the geometry being considered for a particular application, comparisons of data obtained from the vortex meter and other devices such as turbines might establish superiority of one or the other device. Generally, however, the vortex meter probably would have the disadvantage of producing an intermittent signal and requiring high stream velocities to work in two-phase flow.

REFERENCES

1. D. G. Thomas et al., *Quarterly Progress Report on Blowdown Heat Transfer Separate Effects Program for January–March 1978*, NUREG/CR-0133 (ORNL/NUREG/TM-205) (July 1978), pp. 13–15.

2. J. D. White et al., *Quarterly Progress Report on Blowdown Heat Transfer Separate Effects Program for October–December 1979* (to be issued).

3. K. G. Turnage et al., *Advanced Two-Phase Flow Instrumentation Program Quarterly Progress Report for July–September 1978*, NUREG/CR-0686 (ORNL/NUREG/TM-309) (May 1979), pp. 4–5.

4. T. Oshinowo and M. E. Charles, "Vertical Two-Phase Flow, Part I. Flow Pattern Correlations," *Can. J. Chem. Eng.* 53: 25 (1974).

5. G. B. Wallis, *One-Dimensional Two-Phase Flow*, McGraw-Hill, New York, 1969.

6. K. G. Turnage and C. E. Davis, *Advanced Two-Phase Instrumentation Program Quarterly Progress Report for July–September 1979*, NUREG/CR-1092 (ORNL/NUREG/TM-357) (March 1980).

7. K. G. Turnage et al., *Advanced Two-Phase Flow Instrumentation Program Quarterly Progress Report for January–March 1979*, NUREG/CR-0847 (ORNL/NUREG/TM-331) (September 1979), pp. 34–35.

BLANK PAGE

NUREG/CR-1346
ORNL/NUREG/TM-382
Dist. Category R2

Internal Distribution

1. R. L. Anderson
2. M. E. Bagwell
3. C. Brashear
4. S. K. Combs
5. W. B. Cottrell
6. W. G. Craddick
7. C. E. Davis
8. I. T. Dudley
9. B. G. Eads
10. D. K. Felde
11. J. E. Hardy
12. M. B. Herskovitz
13. H. W. Hoffman
14. A. F. Johnson
15. R. N. McGill
16. G. N. Miller
17. C. Mossman
18. C. B. Mullins
19. F. R. Mynatt
20. J. L. Rich
21. M. J. Roberts
22. J. A. Stevens
23. D. G. Thomas
24. R. H. Thornton
25. H. E. Trammell
26. K. G. Turnage
27. ORNL Patent Office
28-29. Central Research Library
30. Document Reference Section
31-32. Laboratory Records Department
33. Laboratory Records Department (RC)

External Distribution

34-41. Director, Division of Reactor Safety Research, Nuclear Regulatory Commission, Washington, DC 20555
42. Director, Reactor Division, DOE, ORO
43. Office of Assistant Manager, Energy Research and Development, DOE, ORO
44-48. Director, Reactor Safety Research Coordination Office, DOE, Washington, DC 20555
49-50. Technical Information Center, DOE
51-410. Given distribution as shown in category R2 (10-NTIS)